



# Euler–Bernoulli elastic beam models of Eringen’s differential nonlocal type revisited within a $C^0$ –continuous displacement framework

A. A. Pisano · P. Fuschi · C. Polizzotto

Received: 30 December 2020 / Accepted: 15 April 2021

© The Author(s) 2021

**Abstract** A theory of the Eringen’s differential nonlocal beams of (isotropic) elastic material is prospected independent of the original integral formulation. The beam problem is addressed within a  $C^0$ –continuous displacement framework admitting slope discontinuities of the deflected beam axis with the formation of bending hinges at every cross section where a transverse concentrated external force is applied, either a load or a reaction. Concepts sparsely known from the literature are in this paper used within a more general context, in which the beam is envisioned as a macro-beam whose microstructure is able to take on a size dependent initial curvature dictated by the loading and constraint conditions. Indeed, initial curvature seems to be an effective analytical tool to inject size effects into micro- and nano-beams. The proposed theory is applied to a set of benchmark beam problems showing that a softening behaviour is always predicted without the appearance

of paradoxical situations. Comparisons with other theories are also presented.

**Keywords** Nonlocal elasticity · Beam theory · Euler–Bernoulli beam · Microstructure in beams · Paradoxes in beams

## 1 Introduction

Eringen [1] proposed a method to solve integro-differential elasticity problems by means of a differential equation whose Green function coincides with the kernel of the integral equation. Eringen et al. [1–7] mainly applied the proposed differential method to problems with unbounded domains (as for instance wave propagation, crack tip singularities, dislocation analysis problems) whereby the asymptotic conditions at infinity, featured by evanescent values of the response functions, make the differential and the integral methods lead to the same solution. In the case of bounded domains, the differential method-based solution may coincide with the integral method-based one but only if the former solution satisfies—in addition to the standard boundary conditions—some extra nonlocality boundary conditions dictated by the integral method-based solution. This latter assessment is the result of recent research work within beam mechanics [8, 9], though roots of it were already

---

A. A. Pisano (✉) · P. Fuschi  
Department PAU, University Mediterranea of Reggio Calabria, Via Dell’Università 25,  
I-89124 Reggio Calabria, Italy  
e-mail: aurora.pisano@unirc.it

P. Fuschi  
e-mail: paolo.fuschi@unirc.it

C. Polizzotto  
Department of Engineering, University of Palermo, Viale delle Scienze, I-90128 Palermo, Italy  
e-mail: c.polizzotto@unipa.it; c.polizzotto@inwind.it

known within the mathematical world of integral equation theories [10].

Always with reference to bounded domains, let us recall that, on the one hand, the Eringen's differential method applied to a (fully) nonlocal Euler–Bernoulli (EB) beam model leads to a fourth order governing differential equation in the beam deflection  $w$  as [11]

$$w''''(x) = \frac{1}{D} [p(x) - \ell^2 p''(x)] \quad (0 < x < L) \quad (1)$$

here the primes denote derivatives with respect to the abscissa  $x$ , whereas  $D = EI =$  bending stiffness,  $p(x) =$  distributed load,  $\ell =$  nonlocality parameter. Equation (1), together with the inherent four standard boundary conditions, leads to a unique solution of the beam problem, but this solution is generally different from the solution of the nonlocal integral problem due to the impossibility to accommodate the mentioned extra boundary conditions [8, 9] (a sixth order differential equation would be needed to this purpose). This means that the Eringen's differential nonlocal method, though different from the nonlocal integral method, possesses a capacity of its own to predict size effects. These effects, arising from the existence of a length scale parameter ( $\ell$ ), make the response of the nonlocal beam exhibit either an increased stiffness feature (stiffness hardening, or simply stiffening), or instead a decreased stiffness feature (stiffness softening, or simply softening), the more the larger is  $\ell$ . Therefore the mentioned Eringen's method constitutes a method apart in which size effects are carried in by the applied distributed load, but the properties of this method are perhaps not well understood yet.

On the other hand, the mentioned nonlocality boundary conditions read as [8]

$$M(0) - \ell M'(0) = M(L) + \ell M'(L) = 0 \quad (2)$$

These, being in evident contrast with the boundary equilibrium conditions, cannot be satisfied and therefore the integral method likely does not admit a solution; in other words, the governing integral equation constitutes a Fredholm integral equation of the first kind, known to lead to a ill-posed boundary-value problem with a multiple solution, or no solution at all [10].

Peddieon et al. [11] first used the Eringen's differential method to address nonlocal beams simulating sensor and actuator devices within nanotechnologies, using for this purpose (1) in association with

the standard boundary conditions. It was found that Eq. (1) leads to a (unique) solution which predicts size effects of different types, either softening or stiffening, with increasing  $\ell$ , apparently without a precise rule. It was also found the existence of paradoxical beam cases, like the cantilever beam under a tip concentrated load, in which the obtained solution coincides with the classical solution, namely no size effects are predicted by the obtained solution. Another paradoxical case is the cantilever beam under uniform load which is usually referred to as a stiffening beam case, but surprisingly no mention is given from the literature about the beam's tendency to deform raising up against the applied load at higher values of the nonlocality parameter. Several other paradoxical beam cases were reported in the literature [9, 17, 25, 39].

The work by Peddieon et al. [11] stimulated a large amount of research which essentially developed along two streams. A first stream includes a huge amount of works in which the differential method is used to solve bending, buckling and vibration problems for nonlocal beams and plates, for which we make reference to the review papers [12–14]. The other stream includes works in which the inconsistencies of the nonlocal integral and differential theories are in some way overcome, often by modifying the constitutive model. The two-phase local/nonlocal constitutive model previously prospected by Eringen [4] and subsequently discussed by Polizzotto [15], was used either within the integral formulation with which the governing equation turns out to be a Fredholm integral equation of the second kind [16–20], or within the differential formulation with which the governing equation is a sixth order differential equation and thus all the boundary conditions (including the extra nonlocality ones) were accommodated [21–24]. A hybrid constitutive model in which the nonlocal integral model is mixed with the strain gradient one—often also called “nonlocal strain gradient” model—was advanced by [25], then developed by [26–30], whereby a constitutive integral equation was used, having as driving variables the strain and strain gradient. A third group of works operates with the Eringen's differential constitutive model itself and reports solutions in which the beam deflection has slope discontinuities at points of application of concentrated loads with size effects in all beam cases, including the so-called paradox cases [31–33]. In addition, a bending hinge was

introduced by [33] at every clamped end(s) of the beam as well as within the beam axis, with which bending hinge lattice based solutions were provided.

The last quoted papers [31–33] provide solutions of the differential nonlocal beam problem out of the usual continuity framework of elasticity theory, with the incorporation of bending hinges; all this by remaining within the original Eringen’s nonlocal differential constitutive model. The obtained beam deflections turn out to be size dependent in all cases, including the paradoxical cases. Indeed, this result seems to be the best one for its capacity to better understand the Eringen’s differential nonlocal beam model and to solve the paradox beam cases. However, a constitutive-like relationship between the bending hinge mechanism and the related concentrated load, valid also for hinges located at the beam constrained end(s), is still lacking, hence the paradoxical beam cases seem to be not completely solved yet.

In the following, we intend to reconsider and rediscuss the above issues of the literature, in the purpose to build a coherent theory for nonlocal beams governed by Eq. (1), but useful to predict size effects without paradoxes, nor other drawbacks.

### 1.1 Objectives of the present work

In the present paper our concern will be the differential Eq. (1) with the appropriate four standard boundary conditions. The solution of Eq. (1) is the response of the nonlocal beam to the load  $p$  augmented by an additional fictitious *size dependent* load  $p_{(0)} = -\ell^2 p''(x)$ . However, by the existence of paradox cases we know that the simulation of size effects by the extra load  $p_{(0)}$  is not always effective, at least within the classical framework of continuous displacement solutions. Since  $p\ell^2/D$  is dimensionally an inverse length, we may interpret this latter term to be proportional to a *size dependent initial (inelastic) curvature*, say  $\chi_{(0)}$ , so that (1) may be rewritten in the form

$$w''''(x) = \frac{1}{D}p(x) - \chi''_{(0)}(x) \quad (0 < x < L) \tag{3}$$

In this way the solution turns out to be the response of the beam to the load  $p$  and to the initial curvature  $\chi_{(0)}$  carrying in size effects. The passage from (1) to (3) is more than a formal transformation, because the

constitutive-like relation between  $\chi_{(0)}$  and  $p$  holds true even if the load is a concentrated force  $P$ , no matter if active or reactive, in which case  $\chi_{(0)}$  transforms into the relative rotation  $\Theta$  of a bending hinge, with a consequent wider class of state variables to describe the beam strain/stress states. All this can be reasonably cast within the mechanics framework of a beam whose microstructure undergoes an initial (inelastic) curvature  $\chi_{(0)}$  leading to solution displacements belonging to the class of  $C^0$ –continuous functions. Furthermore, the so obtained  $C^0$  solutions always resort to a softening behavior of the beam model, without paradoxes, nor other behavioral shortcomings, which means that the Eringen’s differential nonlocal method correspondingly gains the effectiveness of a consistent size effect analysis method.

The theory proposed here above recalls an analogy principle known from the literature [34]. According to this principle, the response of a nonlocal EB beam subjected to a distributed load  $p(x)$  computed through the Eringen’s differential nonlocal method—that is, solving (1)—coincides with the response of the same beam considered of local type and subjected—in addition to the load  $p(x)$ —to the inelastic curvature  $\chi^{in}(x) \equiv \chi_{(0)}(x)$ . The validity of this principle is here confirmed and extended to a wider context whereby concentrated forces, either active or reactive, are also considered among the external actions, whereas bending hinges are correspondingly considered as a particular manifestation of the inelastic deformation of the beam.

The outline of the subsequent developments within this paper are as follows. In Sect. 2, the beam model with microstructure is presented together with the concept of initial (inelastic) curvature taken on by the microstructure, along with the concept of bending hinge forming up at any cross section where a concentrated load is applied (but no discontinuity of the deflection curve is generated by a concentrated couple). In Sect. 3, the solution method is presented. Section 4 is dedicated to the application of the proposed theory, as well as to comments and comparisons. Conclusions are drawn in Sect. 5.

The notation will be defined in the text at the first appearance of the related symbols.

## 2 EB beam model with microstructure

As explained in the preceding section, the Eringen’s differential nonlocal EB beam model is based on a Helmholtz differential equation whose Green function coincides with the kernel function of the related integral constitutive equation. This basic Helmholtz equation may be cast as

$$M(x) - k\ell^2 M''(x) = D\chi(x) \tag{4}$$

where  $\chi(x)$  denotes the beam’s curvature and  $k$  is a (dimensionless) constant ( $0 < k < 1$ ). Accounting for the equilibrium equation,  $M''(x) + p(x) = 0$ , (4) loses its differential character and takes on an algebraic form as

$$M(x) + M_{(0)}(x) = D\chi(x) \tag{5}$$

where  $M_{(0)}(x) := k\ell^2 p(x)$  and thus the size dependence of (4) is saved through the initial bending moment  $M_{(0)}$  carrying in size effects.

A further transformation of (5) is obtained by introducing the quantity

$$\chi_{(0)}(x) := \frac{M_{(0)}(x)}{D} = \frac{k\ell^2}{D} p(x) \tag{6}$$

which coincides with the *initial (inelastic) curvature* mentioned before. Then, (5) can be rewritten in the form

$$M(x) = D \underbrace{[\chi(x) - \chi_{(0)}(x)]}_{\chi_{(e)}} = D\chi_{(e)}(x) \tag{7}$$

Since the magnitude of  $\chi_{(0)}$  increases with  $k$ , this constant characterizes the relative deformation of the microstructure with respect to the continuum, thus  $k$  is referred to as the *compliance coefficient* of the microstructure. For  $k \rightarrow 0$  it is  $\chi_{(0)}(x) \equiv 0$ , that is, no relative deformation of the microstructure is allowed to occur and Eq. (7) takes on the form of classical elasticity correspondingly, i.e.  $M(x) = D\chi(x)$ .

Equation (7) is the constitutive equation of an EB beam model with microstructure, whereby the bending moment  $M$  is proportional to the net (elastic) curvature  $\chi_{(e)} := \chi - \chi_{(0)}$ , difference between the total (compatible) curvature  $\chi = -w''$  and the initial (inelastic) curvature  $\chi_{(0)}$ . Equation (7) recalls an analogous relation given by [34] within an analogy principle,

but here (7) has a wider application domain involving concepts as concentrated forces, either active or reactive, and concomitant bending hinges with consequent slope jumps in the deflection curve  $w(x)$ .

Also, the bending hinge herein introduced appeals to the plastic hinge of limit analysis of beam structures in bending, but these two types of hinges are conceptually different from each other. In fact, a plastic hinge obeys a threshold law and is irreversible, whereas in contrast a bending hinge obeys a one-to-one reversible load-curvature law (6) which is comparable to a *thermal-like* law, but not to a Hooke law whereby deformation is related to internal forces, as in (7).

As a rule, we shall operate taking  $k$  somewhere within the interval (0, 1), but a precise criterion to calibrate the value of  $k$  is lacking for the moment. Heuristically, we may just conjecture that the microstructure’s relative deformation with respect to the macro-beam, and thus the  $k$  coefficient as well, be the smaller the higher is the hyperstatic degree of the beam, such that  $k$  may be fixed, for instance, as  $k \simeq 1/2$  for a statically determinate beam, and  $k \simeq 1/4$  for a fully clamped beam.

### 2.1 Microstructure

The beam’s microstructure is conceived as a continuous set of micro-cell elements as in [35, 36]. Here the cells are one-dimensional beam-like (local-type) elements of equal length, say  $2d$ , every element being capable to deform with respect to the beam matrix. The generic element is appended to the beam matrix, for instance having the centroid points of the end cross sections simply supported upon the beam matrix (segment a-b in Fig. 1). The term “macro-beam” is used here with the same meaning as the term “continuum” within  $3D$ , that is, to indicate the beam together with the microstructure; whereas the term “beam matrix” indicates what remains of the macro-beam after removing the microstructure.

The load  $p$  acts in a two-fold manner, namely: i) Transmitted to the cell elements through the macro-beam,  $p$  acts as a thermal-like load inducing an *initial (inelastic) curvature*  $\chi_{(0)} = k\ell^2 p/D$  of the cell elements in accord with (6); ii) The load  $p$  also induces—through the bending moment  $M$ —a *net (elastic)*

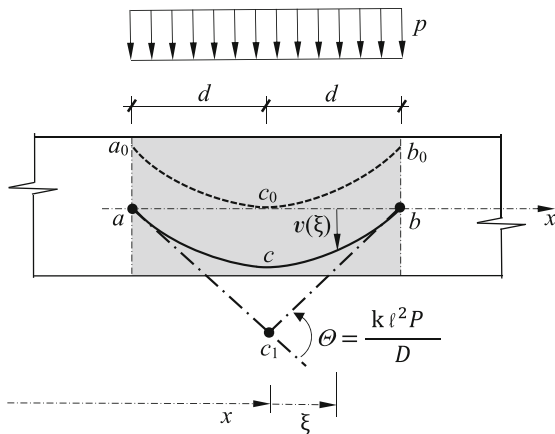


**Fig. 1** Geometrical sketch illustrating a beam-like cell element a-b, which is simply supported by the beam matrix. The load  $p$  transmits itself through the macro-beam to the micro-structure causing the beam element to undergo an initial pre-strained curvature  $\chi_{(0)} = (k\ell^2/D)p$ , whereas the macro-beam deforms according to the constitutive law  $M = D(\chi - \chi_{(0)})$

curvature  $\chi_{(e)}$  of the macro-beam itself in accord with (7).

Assuming  $p(x + \xi) \simeq p(x)$  within every cell,  $\chi_{(0)}$  can there be treated as constant hence the initial deflection of the generic cell—written to within a rigid translation—is given by

$$v(\xi) = \frac{1}{2}k\ell^2p(d^2 - \xi^2)/D, \quad (-d \leq \xi \leq d) \tag{8}$$

which describes the parabola a-c-b of Fig. 1.

As  $v(0) = \frac{1}{2}k\ell^2pd^2/D$ , an upward translation of the solid curve a-c-b opposite to  $v(0)$  leads to the dashed curve  $a_0-c_0-b_0$  of equation

$$v_0(\xi) = v(\xi) - v(0) = -\frac{1}{2}k\ell^2p\xi^2/D \tag{9}$$

This curve is the initial pre-strained configuration of the cell which after application of the load  $p$  will adhere to the axis of the beam matrix, so losing its initial deformation.

The relative (anticlockwise) rotation of the end cross sections of the beam-like cell in the initial deformation state is given by

$$\Theta = -[v'(\xi)]_{-d}^{+d} = \frac{k\ell^2}{D}2dp = \Phi P \tag{10}$$

where  $P = 2dp$  is the total (downward) load applied upon the cell, whereas  $\Phi = k\ell^2/D$  is a constant featuring the compliance of the hinge. On letting  $p$

and  $d$  vary, but keeping  $P$  fixed,  $\Theta$  remains constant even for  $d \rightarrow 0$  and  $p \rightarrow \infty$ , it therefore holds good also in the presence of a concentrated load of intensity  $P$ . Notably, (10) applies to all the cell elements of the beam, including those located at the beam ends where there may exist a constraint giving rise to a reacting (transverse) concentrated force.

It is worthwhile to observe that in virtue of (10), which expresses  $\Theta$  as the jump of the first derivative of the (small) deflection  $v$  of the inherent beam-like cell, the hinge relative rotation  $\Theta$  must be of the same order of magnitude as twice that of  $v'$ ,  $\mathcal{O}(|\Theta|) \approx 2\mathcal{O}(|v'|)$ . In other words,  $\Theta$  must satisfy the inequality

$$|\Theta| = \frac{k|P|\ell^2}{D} < 1 \tag{11}$$

We shall return to this point next (Sect. 4.5).

### 2.2 Micro-beam

For  $d \rightarrow 0$ , the continuous beam-like cell system can be interpreted as a *micro-beam* possessing the same properties of the cell system. Namely, it undergoes an initial inelastic (thermal-like) curvature  $\chi_{(0)}(x) = k\ell^2p(x)/D$  at points  $x$  where a distributed load is applied, but a relative rotation  $\Theta_i = k\ell^2P_i/D$  (bending hinge) at points  $x_i$  where a concentrated load  $P_i$  is applied. As shown in next subsection, loading couples, either distributed or concentrated, do not cause effects upon the microstructure, their possible presence is thus ignored for the moment.

The above is illustrated in Fig. 2, where the macro-beam  $AB$  is subjected to concentrated loads  $P_1$  and  $P_2$  at points  $C_1, C_2$ , respectively, to a uniform loop  $p$  distributed within  $C_1$  and  $C_2$ , along with the concentrated (upward) reacting forces  $V_A$  and  $V_B$  at the ends  $A, B$ , respectively. Whether the end cross sections are clamped or simply supported is irrelevant for the present reasoning. The initial deformation  $\chi_{(0)}$  of the micro-beam is—to within a rigid motion—uniquely described by a (conventional) initial deflection of the beam in the form of a polyline (with a parabolic side under the uniformly distributed load) like the polyline  $aA'C_1c C_2B'b$  of Fig. 2, showing as many hinges as the number of concentrated forces. Note that this polyline is the effect of the initial deformation upon the beam rendered statically determinate. This implies that in general no rigid motion can exist such as to

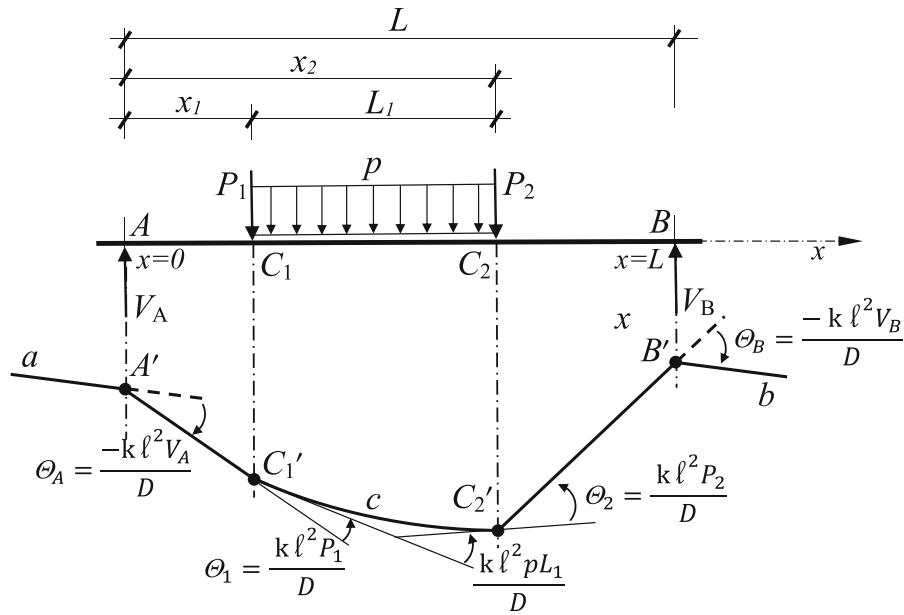


**Fig. 2** Geometrical sketch showing a beam subjected to two concentrated loads  $P_1, P_2$  at points  $C_1, C_2$ , respectively, to a uniform load  $p$  distributed within  $C_1$  and  $C_2$ , along with the concentrated reacting forces at the constrained ends  $A, B$  where non-zero bending moments are allowed to occur. The initial pre-strained deformation includes four bending hinges at points  $A, C_1, C_2, B$ . Since  $V_A + V_B - P_1 - P_2 - pL_1 = 0$ , then the

relative rotation of the end outer cross sections must be vanishing, therefore the (conventional) initial configuration of the beam is a polyline like  $aA'C_1'cC_2'bB'$ , with extreme sides  $aA'$  and  $B'b$  parallel to each other and a parabolic side under the uniformly distributed load  $p$

make the initial deflection line compatible with the beam's constraints at  $A$  and  $B$ , except that the beam is statically determinate. Since by global equilibrium  $V_A + V_B - P_1 - P_2 - pL_1 = 0$ , it results that *the relative rotation of the beam ends is zero*, that is, the end sides  $aA'$  and  $B'b$  of the polyline must be parallel to each other.

$V_A$  and  $V_B$  must be evaluated through equilibrium considerations, as better explained shortly in Sect. 4.

### 2.3 No displacement jump under a concentrated couple

The features of the micro-beam illustrated above do not consider the possible existence of concentrated couples within the loading upon the beam. Here we show that concentrated couples do not produce any discontinuity of the micro-beam initial configuration. For this purpose, let the macro-beam be subjected to two concentrated loads, namely a downward load  $P$  at  $x_0 - e$  and an upward load  $P$  at  $x_0 + e$ , Fig. 3. The initial configuration of the beam is the trilateral line  $abcd$  with  $ab$  parallel to  $cd$  and the bending hinges at

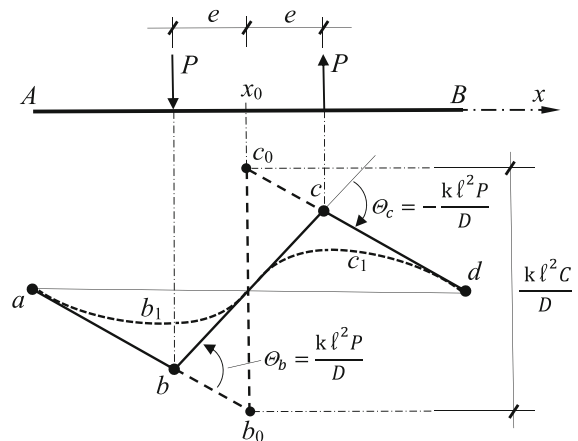


**Fig. 3** Geometrical sketch used to show that no discontinuity is allowed to arise at a point where a concentrated couple is applied, which is a direct consequence of the shear rigidity of the EB beam model

the application points of the concentrated loads. On letting  $e \rightarrow 0, P \rightarrow \infty$ , but  $2eP = C = \text{constant}$ , at the limit the trilateral line  $abcd$  tends to the broken line  $ab_0c_0d$ . The transverse segment  $b_0c_0$  of length  $\ell^2 C/D$

represents a displacement jump at  $x_0$  due to the concentrated (anticlockwise) couple  $C$  applied at  $x_0$ . Since this latter deformation mechanism is of pure shear nature, and since shear strain is forbidden within the context of the present EB beam model, it follows that the initial configuration of the micro-beam cannot take on the broken form  $ab_0c_0d$ , but it instead will be some continuous line (as e.g. the dotted line  $b_1c_1$  of Fig. 3). Therefore, concentrated couples are allowed to play as external actions and thus to have an influence on the beam’s response, but they do not produce effects upon the microstructure.

### 3 The solution method

For a better understanding of the present method, it may be useful to recall that the boundary ends of a nonlocal beam must be thought of as two boundary layers each of small length, say  $\varepsilon$ , such that the effective length of the macro-beam is  $L + 2\varepsilon$  and the beam ends are located at  $x = -\varepsilon$  and  $x = L + \varepsilon$ . Also, differentiations must be intended in a distribution sense.

For this purpose, the symbology exploited by [33, 37] is adopted, in which a concentrated force  $P$  applied at a point  $x_0$  is transformed into a distributed load using a Dirac delta as  $P\delta(x - x_0)$ . Furthermore, the symbol  $\langle \cdot \rangle$  is the Macaulay symbol, that is,  $\langle u \rangle = (u + |u|)/2 = uH(u)$ , whereas  $H(\cdot)$  is the Heaviside symbol, namely  $H(x) = 1$  if  $x > 0$ ,  $H(x) = 0$  otherwise, such that  $\delta(x) = H'(x)$ ,  $H(x) = \langle x \rangle'$ .

The beam model under consideration obeys the constitutive Eq. (7) which, after a double differentiation and recalling that  $\chi = -w''$ , leads to the displacement governing Eq. (3). As an illustrative example we consider a simple beam of length  $L$  subjected to a distributed load  $p(x)$ , to concentrated loads  $P_i$  ( $i = 1, \dots, m$ ) applied at points  $x_i$  and to a concentrated couple  $C_0$  at  $x_0$ ,  $0 < x_0 < L$ . The beam has some constraints at the ends giving rise to (upwards) concentrated reaction forces  $V_A, V_B$ . The solution of the beam problem for assigned static loads is derived through Eq. (3) here reported again in the following shape, where the presence of concentrated forces and couples is explicitly indicated through the Dirac delta distribution  $\delta$ , namely,

$$w''''(x) = \frac{1}{D}p(x) + \frac{1}{D} \left[ \sum_{i=1}^m P_i \delta(x - x_i) + C_0 \delta'(x - x_0) \right] - \chi''_{(0)}(x) \tag{12}$$

By (7), the bending moment  $M(x)$  associated to (12) is

$$M(x) = -Dw''(x) - D\chi_{(0)}(x) \tag{13}$$

Moreover, as stated before, the initial curvature  $\chi_{(0)}$  is uniquely determined from the external applied forces, either active or reactive. Therefore, we can write  $\chi_{(0)}(x)$  as

$$\chi_{(0)}(x) = \underbrace{\frac{k\ell^2}{D}p(x)}_{\substack{\text{distributed} \\ \text{initial} \\ \text{curvature}}} + \underbrace{\frac{k\ell^2}{D} \left[ \sum_{i=1}^m P_i \delta(x - x_i) - V_A \delta(x) - V_B \delta(x - L) \right]}_{(m+2)\text{bending hinges}} \tag{14}$$

Equation (14) predicts a bending hinge at every point where a concentrated force, either active or reactive, is applied, therefore the couple  $C_0$  is not there involved. The reactive forces  $V_A$  and  $V_B$  are given by

$$V_A = M'(0^+), \quad V_B = -M'(L^-) \tag{15}$$

and satisfy the global equilibrium equation

$$V_A + V_B = \sum_{i=1}^m P_i + \int_0^L p(x)dx \tag{16}$$

Next, through the relation  $\chi_{(0)}(x) = -w''_{(0)}(x)$ , Eq. (14) can be integrated to get what can be called *conventional initial deflection* of the beam, namely,

$$w_{(0)}(x) = \frac{k\ell^2}{D} \left[ V_A \langle x \rangle + V_B \langle x - L \rangle - f''(x) - \sum_{i=1}^m P_i \langle x - x_i \rangle \right] \tag{17}$$

where  $f(x)$  is a particular function satisfying the equation  $f''''(x) = p(x) \quad \forall x \in (0, L)$ . Equation (17) gives—to within a rigid motion—the displacement effects produced by the application of the initial curvature upon the beam rendered statically determinate.

Next, substituting (14) into (12) and by integration of (12) we can write:

$$\begin{aligned}
 w(x) &= \frac{1}{6}C_1x^3 + \frac{1}{2}C_2x^2 + C_3x + C_4 \\
 &\quad + \frac{1}{D} \left[ f(x) + \frac{1}{6} \sum_{i=1}^m P_i \langle x - x_i \rangle^3 \right] \\
 &\quad + \frac{C_0}{2D} \langle x - x_0 \rangle^2 + w_{(0)}(x) \\
 &= \frac{1}{6}C_1x^3 + \frac{1}{2}C_2x^2 + C_3x + C_4 \\
 &\quad + \frac{1}{D} \left[ f(x) - k\ell^2 f''(x) \right] + \frac{C_0}{2D} \langle x - x_0 \rangle^2 \\
 &\quad + \frac{1}{6D} \sum_{i=1}^m P_i \langle x - x_i \rangle^3 \\
 &\quad + \frac{k\ell^2}{D} \left[ V_A \langle x \rangle + V_B \langle x - L \rangle - \sum_{i=1}^m P_i \langle x - x_i \rangle \right]
 \end{aligned} \tag{18}$$

where  $C_1, C_2, C_3, C_4$  are some constants. Substituting (18) into (13) gives

$$\begin{aligned}
 M(x) &= -D(C_1x + C_2) - f''(x) \\
 &\quad - \sum_{i=1}^m P_i \langle x - x_i \rangle - C_0 H(x - x_0)
 \end{aligned} \tag{19}$$

and thus, by (15), we have

$$V_A = -DC_1 - f'''(0), \quad V_B = DC_1 + f'''(L) + \sum_{i=1}^m P_i \tag{20}$$

whereby the global equilibrium of the beam is satisfied, namely,

$$\begin{aligned}
 V_A + V_B &= -f'''(0) + f'''(L) + \sum_{i=1}^m P_i \\
 &= \int_0^L p(x) dx + \sum_{i=1}^m P_i
 \end{aligned} \tag{21}$$

At this point it remains to evaluate the four constants  $C_1, C_2, C_3, C_4$  for which the boundary conditions must be used. The resulting procedure will be illustrated in next section dedicated to applications. What has to be pointed out here is that the applied couple  $C_0$  has an influence on the deflection  $w(x)$  and the bending moment  $M(x)$  of the beam, but not upon the

microstructure’s deformation (both  $\chi_{(0)}$  and  $w_{(0)}$  do not depend on  $C_0$ ).

In concluding the present section, we observe that the proposed method can be extended to beams in vibration and buckling, but this extension is left open for the moment. For easy reference, the beam model governed by the above relations will be called shortly as “ $C^0$ -beam model”.

#### 4 Applications to benchmark beam cases

A few benchmark beam cases are addressed as illustrative examples. The procedure presented in Sect. 3 is followed hereafter.

##### 4.1 Cantilever beam under point load

A cantilever beam is here considered, which is subjected to a concentrated load  $P$  at some intermediate point C as sketched in Fig. 4a. There are two concentrated forces, namely, a downward force  $P$  applied at point C of abscissa  $\bar{x} < L$ , and an upward reacting force, say  $V_A$ , at the left end A. Therefore, there arise two bending hinges at points A and C, respectively, such that the related initial inelastic curvature  $\chi_{(0)}$  reads

$$\chi_{(0)}(x) = \frac{k\ell^2}{D} \left[ -V_A \delta(x) + P \delta(x - \bar{x}) \right] \tag{22}$$

By global equilibrium we have  $V_A = P$ . Equation (22) can be integrated to obtain a conventional initial deflection of the beam  $w_{(0)}(x)$  counterpart of (17), that is,

$$w_{(0)}(x) = \frac{k\ell^2 P}{D} \left[ \langle x \rangle - \langle x - \bar{x} \rangle \right] \tag{23}$$

which is sketched in Fig. 4b (solid line). As the beam is statically determinate, the initial deflection  $w_{(0)}(x)$  is compatible.

The  $C^0$  solution of the beam problem is obtained by integration of the governing differential equation

$$w''''(x) = \frac{1}{D} P \delta(x - \bar{x}) - \chi''_{(0)}(x) \tag{24}$$

together with (13) and taking into account (22) along with the boundary conditions



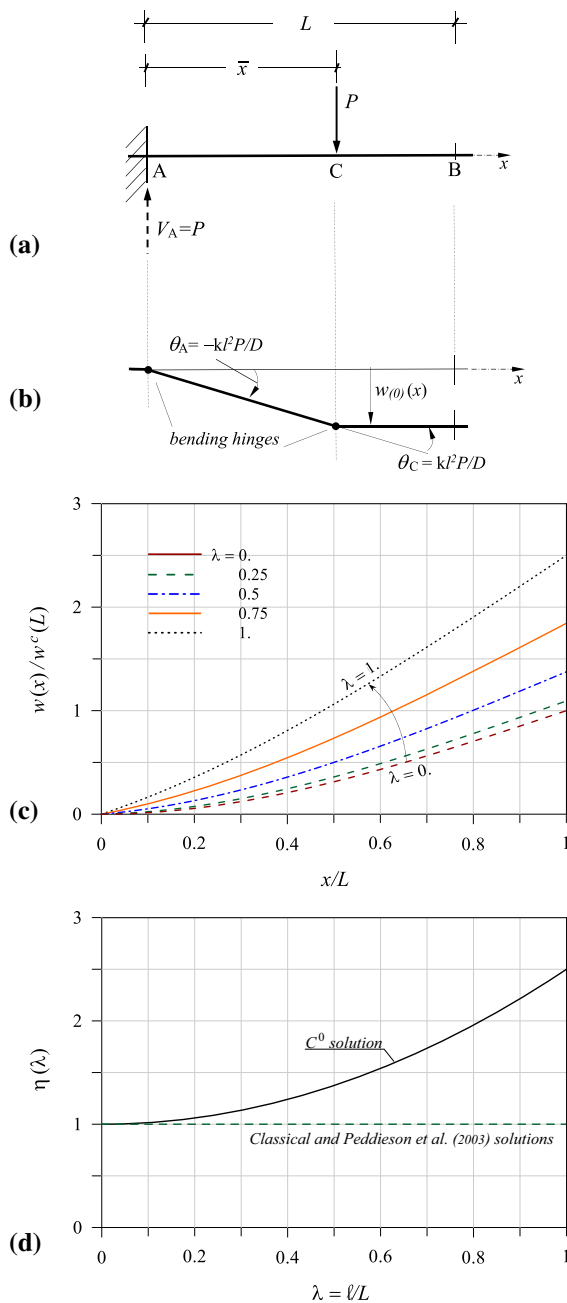


**Fig. 4** Cantilever beam under point load  $P$  at point  $C$  of abscissa  $\bar{x} \leq L$ : **a** Geometric and loading scheme; **b** Conventional (compatible) initial deflection  $w_{(0)}(x)$ ; **c** Normalized  $C^0$  deflection  $w(x)/w_{max}^c$  plotted as a function of  $x/L$  for  $\bar{x} = L$  and different values of  $\lambda = \ell/L = 0., 0.25, 0.5, 0.75, 1.$ ; **d** Normalized maximum  $C^0$  deflection  $\eta(\lambda) = w(L)/w^c(L)$  plotted as a function of  $\lambda$ . (The value  $k = 0.5$  has been used)

$$w(0) = w'(0^-) = 0, \quad M(\bar{x}) = 0, \quad M'(\bar{x}^-) = P \tag{25}$$

Written for the interval  $(0, L)$ , the  $C^0$  deflection proves to be

$$w(x) = \begin{cases} \underbrace{-\frac{P}{6D}x^3 + \frac{P\bar{x}}{2D}x^2 + \frac{k\ell^2 P}{D}x}_{\text{classical solution } w^c(x)} & (0 \leq x \leq \bar{x}) \\ \underbrace{-\frac{P}{6D}\bar{x}^3 + \frac{P}{2D}\bar{x}^2 x + \frac{k\ell^2 P}{D}\bar{x}}_{w^c(\bar{x}) + w_{(0)}(\bar{x})(x-\bar{x})} & (\bar{x} \leq x \leq L) \end{cases} \tag{26}$$

whereas the bending moment is given by

$$M(x) = \begin{cases} -P(\bar{x} - x) & (0 \leq x \leq \bar{x}) \\ 0 & (\bar{x} \leq x \leq L) \end{cases} \tag{27}$$

Since  $w_{(0)}(x)$  is compatible, then we have  $w(x) = w^c(x) + w_{(0)}(x)$ , whereas the bending moment coincides with its classical form.

For  $\bar{x} = L$  (26) and (27) become respectively:

$$w(x) = \frac{P}{D} \left( -\frac{1}{6}x^3 + \frac{L}{2}x^2 \right) + \frac{k\ell^2 P}{D}x \quad (0 \leq x \leq L) \tag{28}$$

$$M(x) = -P(L - x) \quad (0 \leq x \leq L) \tag{29}$$

In Fig. 4c the  $C^0$  solution  $w(x)$  of (28) is reported as a function of  $x/L$ , normalized with respect to the maximum deflection  $w^c(L) = PL^3/3D$  and for different values of  $\lambda = \ell/L$  ( $= 0., 0.25, 0.5, 0.75, 1.$ ). Analogously, in Fig. 4d the normalized maximum  $C^0$  deflection  $\eta := w(L)/w^c(L)$  is plotted as a function of  $\lambda$ . The value  $k = 0.5$  has been used for the plots of Fig. 4c, d. We remark that the solution (26) differs from the analogous solution by [33], where no bending hinge is considered at point  $C$  where the load  $P$  is applied. For  $\bar{x} = L$ , the classical paradox beam case is obtained, but without any paradox therein. A softening behavior is exhibited by the beam ( $\eta(\lambda) > \eta(0) \forall \lambda \neq 0$ ).

#### 4.2 Cantilever beam under uniform load

A cantilever beam under a uniformly distributed load  $p$  is here considered (Fig. 5a), which is usually referred to as the stiffening beam case. There is only one

(upward) concentrated force,  $V_A = pL$  at the clamped end A, hence only one bending hinge at the same point. The initial curvature is expressed as

$$\chi_{(0)}(x) = \frac{k\ell^2}{D} \left[ -pL\delta(x) + p \right] \tag{30}$$

This, by integration, gives the (compatible) conventional initial deflection  $w_{(0)}(x)$ , namely,

$$w_{(0)}(x) = \frac{k\ell^2}{D} \left[ pL\langle x \rangle - \frac{1}{2}px^2 \right] \tag{31}$$

which is reported in Fig. 5b. Proceeding as in the previous case and considering the boundary conditions

$$w(0) = w'(0^-) = 0, \quad M(L) = M'(L) = 0 \tag{32}$$

the  $C^0$  deflection, written for the interval  $(0, L)$ , reads as

$$w(x) = \underbrace{\frac{p}{D} \left[ \frac{1}{24}x^4 - \frac{L}{6}x^3 + \frac{L^2}{4}x^2 \right]}_{\text{classical solution } w^c(x)} + \underbrace{\frac{k\ell^2 p}{2D} (2L-x)x}_{w_{(0)}(x)} \tag{33}$$

which asserts a softening behavior of the beam. Also it is

$$M(x) = -\frac{1}{2}p(L-x)^2 \tag{34}$$

In Fig. 5c the normalized  $C^0$  deflection  $w(x)/w^c(L)$  is plotted as a function of  $x/L$  for different values of  $\lambda = \ell/L$  ( $= 0, 0.25, 0.5, 0.75, 1$ ), whereas in Fig. 5d the maximum  $C^0$  deflection is plotted as a function  $\eta(\lambda)$ . Again the value  $k = 0.5$  has been used. We observe that the  $C^0$  solution (33) coincides with the analogous one by [33], which was derived adding to the classical solution the effects of relaxing the kinematics at the clamped end. Again a softening behavior is exhibited by the beam ( $\eta(\lambda) > \eta(0) \forall \lambda \neq 0$ ).

### 4.3 Clamped-pinned beam under uniform load

Here, a clamped-pinned beam under uniformly distributed load  $p$  is considered (Fig. 6a). As there are two concentrated forces, namely the reactions  $V_A$  and  $V_B$  at the beam ends, there arise two bending hinges correspondingly, hence the initial curvature reads

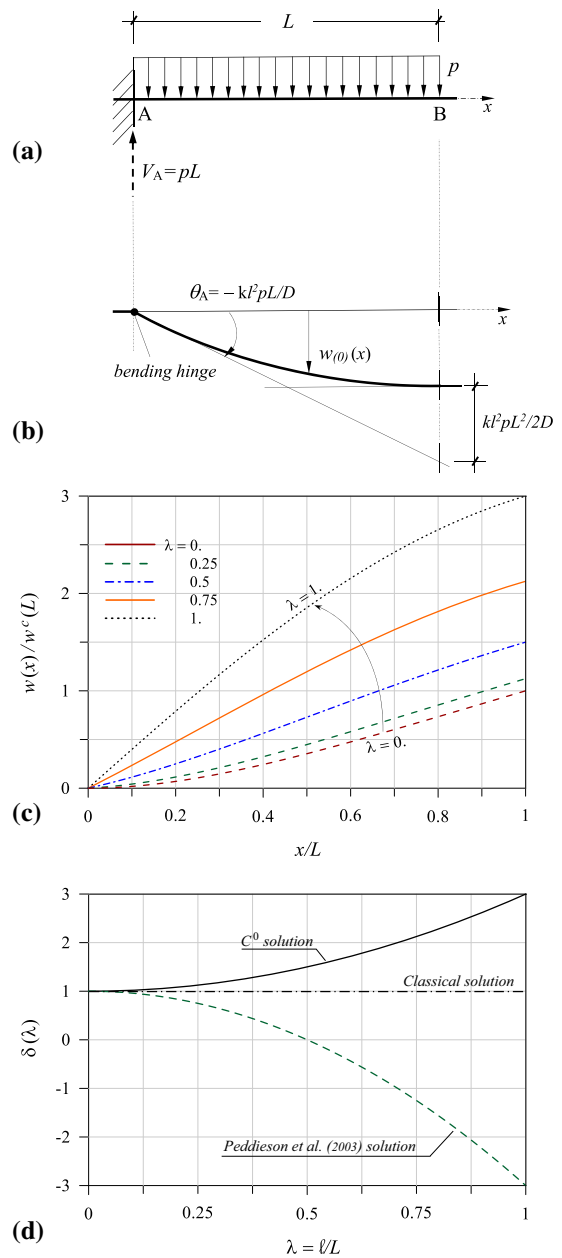


**Fig. 5** Cantilever beam under distributed uniform load  $p$ : **a** Geometric and loading scheme; **b** Conventional (compatible) initial deflection  $w_{(0)}(x)$ ; **c** Normalized  $C^0$  deflection  $w(x)/w^c(L)$  plotted as a function of  $x/L$  for different values of  $\lambda = \ell/L = 0, 0.25, 0.5, 0.75, 1$ ; **d** Normalized maximum  $C^0$  deflection  $\eta(\lambda) = w(L)/w^c(L)$  plotted as a function of  $\lambda$ . (The value  $k = 0.5$  has been used)

$$\chi_{(0)}(x) = \frac{k\ell^2}{D} \left[ p - V_A\delta(x) - V_B\delta(x-L) \right] \tag{35}$$

The related conventional initial deflection proves to be expressed as

$$w_{(0)}(x) = \frac{k\ell^2}{D} \left[ V_A\langle x \rangle + V_B\langle x-L \rangle - \frac{1}{2}px^2 \right] \tag{36}$$

which is plotted in Fig. 6b (solid line). As the beam under consideration is statically indeterminate, the conventional initial deflection  $w_{(0)}(x)$  of (36) is incompatible, since in fact  $w_{(0)}(L) \neq 0$ , though  $w'_{(0)}(0^-) = 0$ . Next, considering the boundary conditions

$$w(0) = w'(0^-) = 0, \quad w(L) = 0, \quad M(L) = 0 \tag{37}$$

by integration of the pertaining governing differential equation we get the  $C^0$  deflection as

$$w(x) = \frac{pL^4}{8D} \frac{1}{1+3k\lambda^2} \left[ -\frac{1}{6}(5+12k\lambda^2)\left(\frac{x}{L}\right)^3 + \frac{1}{2}\left(\frac{x}{L}\right)^2 + (5+12k\lambda^2)k\lambda^2\left(\frac{x}{L}\right) \right] + \frac{pL^4}{24D} \left[ \left(\frac{x}{L}\right)^2 - 12k\lambda^2 \right] \left(\frac{x}{L}\right)^2 \tag{38}$$

and the bending moment  $M(x)$  as

$$M(x) = \frac{pL^2}{8} \frac{1}{1+3k\lambda^2} \left[ (5+12k\lambda^2)\left(\frac{x}{L}\right) - 1 \right] - \frac{pL^2}{2} \left(\frac{x}{L}\right)^2 \tag{39}$$

both of which hold within the interval  $(0, L)$ . For  $\lambda = 0$ , (38) and (39) provide the classical solution. The hinge relative rotation at  $x = 0$  is found to be expressed as

$$\Theta_A = -\frac{pL^3}{D} \frac{(5+12k\lambda^2)}{8(1+3k\lambda^2)} k\lambda^2 \tag{40}$$

In Fig. 6c the  $C^0$  deflection  $w(x)$  is plotted as a function of  $x/L$ , normalized with respect to the maximum classical deflection  $w_{max}^c \approx w^c(L/2)$  and for different values of the scale parameter  $\lambda = \ell/L$  ( $= 0., 0.25, 0.5, 0.75, 1.$ ). Analogously, in Fig. 6d, the normalized maximum  $C^0$  deflection  $w_{max}/w_{max}^c$  is

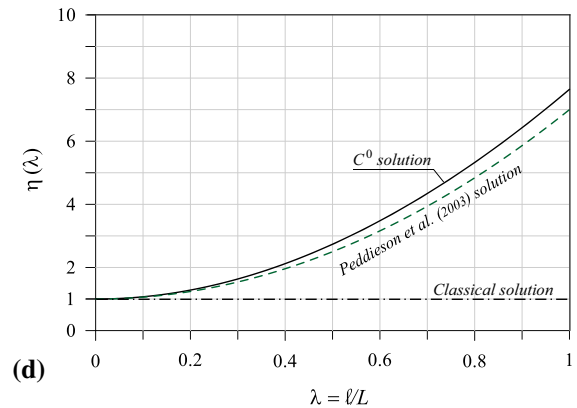
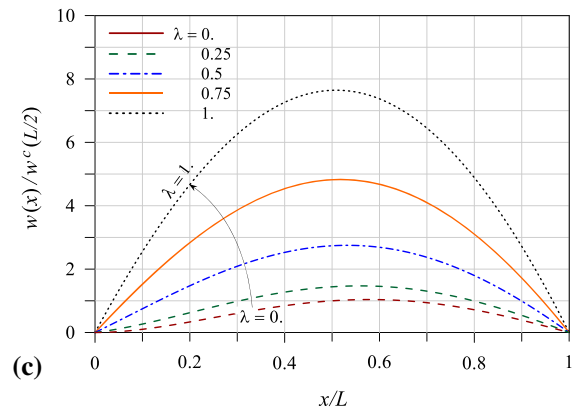
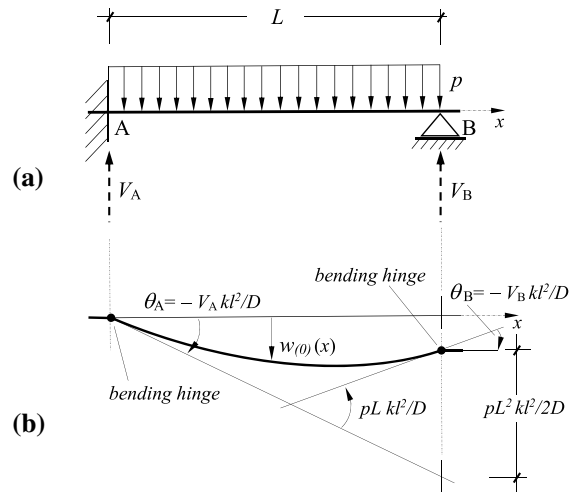


**Fig. 6** Clamped-pinned beam under distributed uniform load  $p$ : **a** Geometric and loading scheme; **b** Conventional (incompatible) initial deflection  $w_{(0)}(x)$ ; **c** Normalized  $C^0$  deflection  $w(x)/w_{max}^c$  plotted as a function of  $x/L$  for different values of  $\lambda = \ell/L = 0., 0.25, 0.5, 0.75, 1.$ ; **d** Normalized maximum  $C^0$  deflection  $\eta(\lambda) = w_{max}/w_{max}^c$  plotted as a function of  $\lambda$ . (The value  $k = 0.25$  has been used)

reported as a function  $\eta(\lambda)$ . It is shown that the  $C^0$  plot exhibits a softening behavior like that of Peddieson et al. [11], but in a slightly more pronounced proportion; for instance for  $\lambda = 0.5$ ,  $\eta_{c^0}(0.5) = 2.74$  while  $\eta_{Pedd}(0.5) = 2.50$ . The value  $k = 0.25$  has been used.

4.4 Clamped-pinned beam under a concentrated load

Here a clamped-pinned beam subjected to a concentrated load  $P$  at  $\bar{x} = L/2$  is considered (Fig. 7a). This time we deal with three concentrated forces, namely the downward force  $P$  at middle point C, along with the (upward) reacting forces  $V_A$  and  $V_B$ . Therefore there arise three bending hinges at the same points and the inherent initial curvature proves to be

$$\chi_{(0)}(x) = \frac{k\ell^2}{D} \left[ -V_A\delta(x) - V_B\delta(x - L) + P\delta\left(x - \frac{L}{2}\right) \right] \tag{41}$$

to which we can associate the (incompatible) conventional initial deflection as

$$w_{(0)}(x) = \frac{k\ell^2}{D} \left[ V_A\langle x \rangle + V_B\langle x - L \rangle - P\langle x - \frac{L}{2} \rangle \right] \tag{42}$$

which is reported in Fig. 7b (solid line). Next, considering the boundary conditions

$$w(0) = w'(0^-) = 0, \quad w(L) = M(L) = 0 \tag{43}$$

and recalling (41), by integration of the governing differential equation the  $C^0$  deflection function  $w(x)$  proves to be

$$w(x) = \frac{PL^3}{16D} \left[ -\frac{11 + 24k\lambda^2}{6(1 + 3k\lambda^2)} \left(\frac{x}{L}\right)^3 + \frac{3}{2(1 + 3k\lambda^2)} \left(\frac{x}{L}\right)^2 + \frac{(11 + 24k\lambda^2)k\lambda^2 x}{1 + 3k\lambda^2 L} \right] + \frac{PL^3}{6D} \begin{cases} 0 & (0 \leq x \leq L/2) \\ \left(\frac{x}{L} - \frac{1}{2}\right)^3 - 6k\lambda^2 \left(\frac{x}{L} - \frac{1}{2}\right) & (L/2 \leq x \leq L) \end{cases} \tag{44}$$

and the bending moment  $M(x)$  as

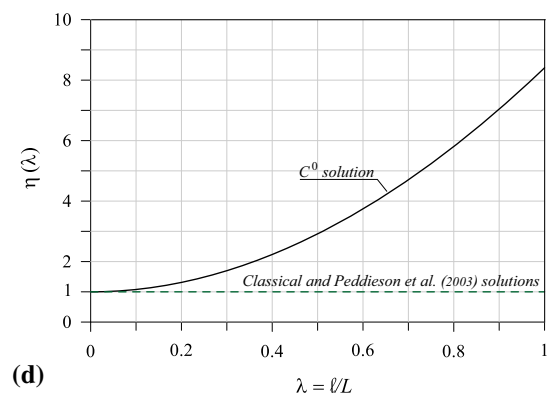
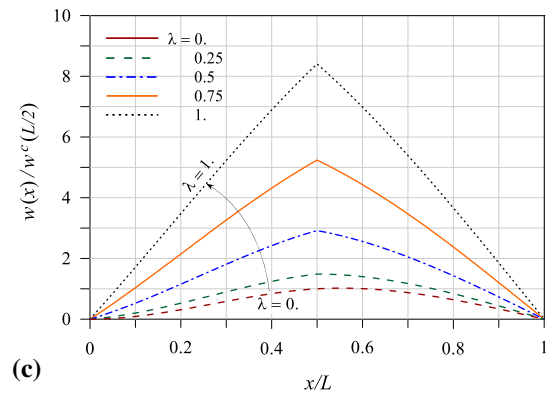
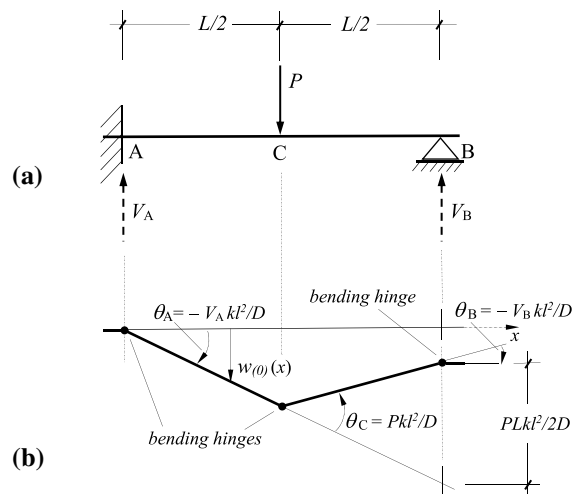


**Fig. 7** Clamped-pinned beam under point load  $P$  at  $L/2$ : **a** Geometric and loading scheme; **b** Conventional (incompatible) initial deflection  $w_{(0)}(x)$ ; **c** Normalized  $C^0$  deflection  $w(x)/w_{max}^c$  plotted as a function of  $x/L$  for different values of  $\lambda = \ell/L = 0., 0.25, 0.5, 0.75, 1.$ ; **d** Normalized maximum  $C^0$  deflection  $\eta(\lambda) = w_{max}/w_{max}^c$  plotted as a function of  $\lambda$ . (The value  $k = 0.25$  has been used)

$$M(x) = \frac{PL}{16} \left[ \frac{11 + 24k\lambda^2 x}{1 + 3k\lambda^2} - \frac{3}{1 + 3k\lambda^2} \right] - \begin{cases} 0 & (0 \leq x \leq L/2) \\ P\left(x - \frac{L}{2}\right) & (L/2 \leq x \leq L) \end{cases} \tag{45}$$

Both (44) and (45) hold for  $0 \leq x \leq L$ ; they recover the respective classic form for  $\lambda = 0$ . The hinge relative rotation at A is given by

$$\Theta_A = -\frac{PL^2}{D} \frac{11 + 24k\lambda^2}{16(1 + 3k\lambda^2)} k\lambda^2 \tag{46}$$

In Fig. 7c the  $C^0$  deflection  $w(x)$  is reported as a function of  $x/L$ , normalized with respect to the  $w^c(L/2)$ , for different values of  $\lambda = \ell/L$  ( $= 0., 0.25, 0.5, 0.75, 1.$ ). Also, in Fig. 7d the normalized maximum  $C^0$  deflection  $w(L/2)/w^c(L/2)$  is plotted as a function  $\eta(\lambda)$ . Both plots of Fig. 7c, d show that the  $C^0$  model exhibits a softening behavior. Again  $k = 0.25$  has been assumed.

#### 4.5 Remarks on the obtained results

The main result of the applications presented above is that in all beam cases a softening behavior of nonlocal gradient beam models is exhibited, without drawbacks of any sort, and this for all loading and constraint conditions. This result is in strong contrast with the outcome from Peddieson et al. [11], where the displacement solution of analogous beam problems was searched for within the classical continuity framework. The work by Peddieson et al. [11] showed that the solution of differential nonlocal beam problems generally indicates a softening behavior of micro- and nano-beams, but that the continuity restriction therein maintained caused dramatic limitations of the size dependent response in some beam cases. For instance, either size effects are not predicted at all whenever the beam is subjected to concentrated loads (as for a cantilever beam under point load), or the beam subjected to uniform load exhibits stiffening effects increasing with the nonlocal scale parameter, the more the larger is this parameter, which leads the beam to deflect upwards against the (downward) load (as in the case of a cantilever beam under uniform load).

As stated before, the examples reported above clearly indicate that the  $C^0$ -continuous solutions of the

fourth order differential equation and boundary conditions indicate a softening behavior for all beam cases without paradoxes and no other shortcomings. Indeed, no paradoxical situations are encountered if one accepts the presence of bending hinges within the context of elastic beams, along with the consequent presence of slope discontinuities. However, as mentioned at the end of Sect. 2.1, the presence of bending hinges carries in limitations as (11) to the amplitude of the hinge relative rotations. The relative rotations  $\Theta_A$  at the left clamped ends of the beam samples worked out before are all of the form

$$\Theta_A = -\zeta(\lambda)k\lambda^2\phi, \quad \phi := \frac{PL^2}{D} = \frac{P(\sqrt{2}L)^2}{2D} \tag{47}$$

where  $P$  denotes the total load applied upon the beam, whereas  $\zeta(\lambda)$  is a case dependent coefficient, that is

$$\zeta(\lambda) = \begin{cases} 1 & \text{Cantilever beam under point load } P \text{ at free end} \\ 1 & \text{Cantilever beam under uniform load } p = P/L \\ \frac{5 + 12k\lambda^2}{8(1 + 3k\lambda^2)} & \text{Clamped-pinned beam under uniform load } p = P/L \\ \frac{11 + 24k\lambda^2}{16(1 + 3k\lambda^2)} & \text{Clamped-pinned beam under point load } P \text{ at } x = \frac{L}{2} \end{cases}$$

This result indicates that  $0 < \zeta(\lambda) \leq 1 \forall \lambda$  (and likely for almost all other beam cases). The factor  $\phi$  may be interpreted as the rotation of the end cross section of a cantilever beam of length  $\sqrt{2}L$  and stiffness  $D = EI$ , subjected to concentrated load  $P$  at the free end. Within the framework of classical linearized elasticity featured by infinitesimal displacements (not too high load  $P$ , nor too small stiffness  $D$ ) we may assume that  $\phi < < 1$ . Therefore we may assert that

$$|\Theta_A| = \zeta(\lambda)k\lambda^2\phi < \phi < < 1 \quad \forall \lambda < 1/\sqrt{k} \tag{48}$$

which obviously can be extended to all bending hinges of the beam. Indeed, the amplitude of the hinge relative rotations is infinitesimal within the present theory. On the other hand, a restriction on the boundedness of  $\lambda$  seems to be in good agreement with an analogous restriction descending from the requirement that the nonlocal continuum model saves its own effectiveness versus atomic lattice models, to which it in fact tends to resort for  $\lambda = \ell/L$  values larger than unit [1, 27, 38]. For the above reasons here we have considered  $\lambda$  values within the interval  $(0, 1)$ .

## 5 Concluding remarks

We have presented a method to solve EB beam models within the framework of  $C^0$ -continuous displacement functions, in which the beam deflection function is allowed to exhibit slope discontinuities at the application points of concentrated forces, either loads, or reacting forces. Concepts as bending hinge and associated relative rotation, which were sparsely advanced within the literature, are here rationally collected within a consistent continuum mechanics framework in which the beam is endowed with a microstructure undergoing an initial (inelastic) curvature carrying in the inherent size dependent effects. The resulting  $C^0$ -beam model leads to a unique solution of the beam problem, featured by a softening behavior for all beam's load and constraint cases, without paradoxical situations or other shortcomings. In contrast with the original Eringen-Peddieon model, the present one may widely be used for size effect analysis of beams in bending, buckling and vibration in a consistent manner.

**Funding** The authors declare that this study did not receive funding.

### Declarations

**Conflict of interest** The authors declare that they have no conflict of interest.

**Open Access** This article is licensed under a Creative Commons Attribution 4.0 International License, which permits use, sharing, adaptation, distribution and reproduction in any medium or format, as long as you give appropriate credit to the original author(s) and the source, provide a link to the Creative Commons licence, and indicate if changes were made. The images or other third party material in this article are included in the article's Creative Commons licence, unless indicated otherwise in a credit line to the material. If material is not included in the article's Creative Commons licence and your intended use is not permitted by statutory regulation or exceeds the permitted use, you will need to obtain permission directly from the copyright holder. To view a copy of this licence, visit <http://creativecommons.org/licenses/by/4.0/>.

## References

- Eringen AC (1983) On differential equations of nonlocal elasticity and solutions of screw dislocation and surface waves. *J Appl Phys* 54(9):4703–4710
- Eringen AC (1972) Linear theory of nonlocal elasticity and dispersion of plane waves. *Int J Eng Sci* 10(5):425–435
- Eringen AC (1977) Edge dislocation on nonlocal elasticity. *Int J Eng Sci* 15:177–183
- Eringen AC (1987) Theory of nonlocal elasticity and some applications. *Res Mech* 21:313–342
- Eringen AC (2002) *Nonlocal continuum field theories*. Springer, New York
- Eringen AC, Kim BS (1974) Stress concentration at the tip of a crack. *Mech Res Commun* 1(4):233–237
- Eringen AC, Speziale CA, Kim BS (1977) Crack tip problem in nonlocal elasticity. *J Mech Phys Solids* 5:339–355
- Polyanin A, Manzhirov A (2008) *Handbook of integral equations*. CRC Press, New York
- Romano G, Barretta R, Diaco M, Marotti de Sciarra F (2017) Constitutive boundary conditions and paradoxes in nonlocal elastic nanobeams. *Int J Mech Sci* 121:151–156
- Tricomi FG (1985) *Integral equations*. Dover Books in Mathematics, UK
- Peddieon J, Buchanan GR, McNitt RP (2003) Application of nonlocal continuum models to nanotechnology. *Int J Eng Sci* 41:305–312
- Eltaher MA, Khater ME, Emam SA (2016) A review on nonlocal elastic models for bending, buckling, vibrations and wave propagation of nanoscale beams. *Appl Math Model* 40:4109–4128
- Rafii-Tabar H, Ghavanloo E, Fazelzadeh SA (2016) Nonlocal continuum-based modeling of mechanical characteristics of nanoscopic structures. *Phys Rep* 638(1):1–97
- Thai H-T, Vo TP, Nguyen T-K, Kim S-E (2017) A review of continuum mechanics models for size-dependent analysis of beams and plates. *Comp Struct* 177:196–219
- Polizzotto C (2001) Nonlocal elasticity and related variational principles. *Int J Solids Struct* 38(42–43):7359–7380
- Khodabakhshi P, Reddy JN (2015) A unified integro-differential nonlocal model. *Int J Eng Sci* 95:60–75
- Fernández-Sáez J, Zaera R, Loya JA, Reddy JN (2016) Bending of Euler-Bernoulli beams using Eringen's integral formulation: A paradox resolved. *Int J Eng Sci* 99:107–116
- Malagù M, Benvenuti E, Simone A (2015) One-dimensional nonlocal elasticity for tensile single-walled carbon nanotubes: a molecular structural mechanics characterization. *Eur J Mech A Solids* 54:160–170
- Fuschi P, Pisano AA, Polizzotto C (2019) Size effects of small-scale beams in bending addressed with a strain-difference based nonlocal elasticity theory. *Int J Mech Sci* 151:661–671
- Pisano AA, Fuschi P, Polizzotto C (2020) A strain-difference based nonlocal elasticity theory for small-scale shear-deformable beams with parametric warping. *Int J Multiscale Comput Eng* 18(1):83–102
- Wang YB, Zhu XW, Dai H-H (2016) Exact solutions for the static bending of Euler-Bernoulli beams using Eringen's two-phase local/nonlocal model. *AIP Adv* 6:085114
- Zhu X, Wang Y, Dai H-H (2017) Buckling analysis of Euler-Bernoulli beams using Eringen's two-phase nonlocal model. *Int J Eng Sci* 116:130–140
- Benvenuti E, Simone A (2013) One-dimensional nonlocal and gradient elasticity: closed-form solution and size effects. *Mech Res Commun* 48:46–51
- Pisano AA, Fuschi P, Polizzotto C (2021) Integral and differential approaches to Eringen's nonlocal elasticity models accounting for boundary effects with applications to beams

- in bending. *Z Angew Math Mech.* <https://doi.org/10.1002/zamm.202000152>
25. Challamel N, Wang CM (2008) The small length scale effect for a nonlocal cantilever beam: a paradox solved. *Nanotechnology* 19(34):345703
  26. Malagù M, Benvenuti E, Duarte CA, Simone A (2014) One-dimensional nonlocal and gradient elasticity: assessment of high order approximation schemes. *Comput Methods Appl Mech Eng* 275:138–158
  27. Lim CW, Zhang G, Reddy JN (2015) A higher-order nonlocal elasticity and strain gradient theory and its applications in wave propagation. *J Mech Phys Solids* 78:298–313
  28. Xu X-J, Wang X-C, Zheng M-L, Ma Z (2017) Bending and buckling of nonlocal strain gradient elastic beams. *Comp Struct* 160:366–377
  29. Faghidian SA (2018) Reissner stationary variational principle for nonlocal strain gradient theory of elasticity. *Eur J Mech A Solids* 70:115–126
  30. Zaera R, Serrano Ó, Fernández-Saéz J (2019) On the consistency of the nonlocal strain gradient elasticity. *Int J Eng Sci* 138:65–81
  31. Wang Q, Shindo Y (2006) Nonlocal continuum models for carbon nanotubes subjected to static loading. *J Mech Math Struct* 1(4):663–680
  32. Wang Q, Liew KM (2007) Application of nonlocal continuum mechanics to static analysis of micro- and nano-structures. *Phys Lett A* 363:236–242
  33. Challamel N, Reddy JN, Wang CM (2016) Eringen's stress gradient model for bending of nonlocal beams. *ASCE J Eng Mech* 142(12):04016095
  34. Barretta R, Marotti de Sciarra F (2015) Analogies between nonlocal and local Bernoulli–Euler nanobeams. *Arch Appl Mech* 85(1):89–99
  35. Mindlin RD (1964) Micro-structure in linear elasticity. *Arch Rat Mech Anal* 16:51–78
  36. Germain P (1973) The method of virtual power in continuum mechanics. Part 2: microstructure. *SIAM J Appl Math* 25(3):556–575
  37. Yavari A, Sarkani S, Reddy JN (2001) On nonuniform Euler–Bernoulli and Timoshenko beams with jump discontinuities: application of distribution theory. *Int J Solids Struct* 38:8389–8406
  38. Reddy JN, Pang SD (2008) Nonlocal continuum theories of beams for the analysis of carbon nanotubes. *J Appl Phys* 103:023511
  39. Li C, Yao L, Chen W, Li S (2015) Comments on nonlocal effects in nano-cantilever beams. *Int J Eng Sci* 87:47–57

**Publisher's Note** Springer Nature remains neutral with regard to jurisdictional claims in published maps and institutional affiliations.